Available online at www.sciencedirect.com
ScienceDirect
Coordination Chemistry Reviews 252 (2008) 233–243
COORDINATION CHEMISTRY REVIEWS
www.elsevier.com/locate/ccr

Review

Revealing the structure of the Mn-cluster of photosystem II by X-ray crystallography

James Barber*, James W. Murray

Division of Molecular Biosciences, Imperial College London, London SW7 2AZ, UK

Received 13 March 2007; accepted 10 August 2007
Available online 19 August 2007

Contents

Abstract

X-ray crystallography has provided details of the location, structure and protein environment of the Mn_4Ca^{2+} cluster which catalyses the light driven, water splitting reaction of photosystem II. However, because of the low resolutions of the crystal structures reported to date, and the possibility of radiation damage at the catalytic centre, the precise position of each metal ion remains a matter of debate. To some extent these problems have been overcome by applying spectroscopic techniques such as Extended X-ray Absorption Fine Structure (EXAFS). The present state of knowledge is reviewed and used to construct two new models for water splitting site. These new models are discussed in terms of the earlier structures.

Keywords: Photosystem II; Mn-cluster; Structure; Protein ligands; X-ray crystallography; Water splitting

1. Introduction

The first hints that manganese is involved in the water splitting-oxygen evolving reaction of photosystem II (PSII) stem back to the work of Pirson [1] who showed that Mn deficiency in the fresh water green alga, *Ankistrodesmus*, inhibited photosynthesis. Following this, similar results were obtained for a wide range of different algae and higher plants [2–4]. It was also demonstrated that the inhibition of photosynthesis could be restored by adding back Mn^{2+} to a suspension of algal cells depleted of this nutrient and that illumination was an absolute requirement for this reactivation (reviewed in [5]). The realisation that Mn was required specifically for the water splitting reaction began with the work of Kessler et al. [6], who noted that Mn deficiency in algae resulted in a reduction in the level of luminescence and this effect coincided with the inhibition

* Corresponding author. Tel.: +44 207 594 5266; fax: +44 207 594 5267.
E-mail address: j.barber@imperial.ac.uk (J. Barber).

0010-8545/$ – see front matter.
doi:10.1016/j.ccr.2007.08.013

of photosynthesis. However they found under the same conditions that the photoreduction of CO_2 using H_2 as an electron source was not inhibited. The explanation of this result became clear with the emergence of the concept of two photosystems acting in series [7] indicating that Mn ions where needed for the oxygen evolving activity of PSII but not for light-induced electron transport through photosystem 1 (PSI) [3,4,8,9]. Work of Blankenship and Sauer [10] showed that the Mn ions were bound to the lumenal surface of PSII and a number of independent studies pointed to a stoichiometry of four Mn ions per PSII reaction centre (reviewed in [11]).

Since then physical techniques such as UV/vis difference absorption spectroscopy [12–15], Electron Paramagnetic Resonance (EPR) spectroscopy ([16] and reviewed in [17,18]) and X-ray spectroscopy [19–21] have clearly indicated that Mn ions play a crucial role in the catalyses of the water splitting reaction leading to the release of protons and electrons and formation of the O=O bond of molecular oxygen. The structural organisation of the Mn-cluster within PSII was however unclear and relied on information derived from Extended X-ray Absorption Fine Structure (EXAFS) spectroscopy [22–25], EPR techniques [17,26–30], Fourier Transfer Infrared (FTIR) spectroscopy [31] and related details derived from synthesis and study of model compounds [32–34]. Although a wide selection of structures were suggested, the most favoured was the "dimer-of-dimer" model consisting of two Mn–di-μ-oxo–Mn groups linked by a Mn–mono-μ-oxo–Mn bond derived from EXAFS [24]. This model was in part based on measured Mn–Mn distances of about 2.7 Å (typical of Mn–di-μ-oxo–Mn bonds) and 3.3 Å (typical of a Mn–mono-μ-oxo–Mn bond). Other structural models were also suggested from EPR studies and comparison with model compounds [30]. However, it was the analysis of Electron Nuclear Double Resonance (ENDOR) and EPR data by Peloquin et al. [17,29], and earlier by Hasegawa et al. [28], that provided a model which seems to be closer to the truth. Based on the strength of spin interactions, it was concluded that the organisation involved three tightly interacting Mn ions with a fourth being less electronically coupled. This 3 + 1 configuration was termed the "dangler" model by Peloquin and Britt [17] and was found to be consistent with that derived from X-ray crystallography (see below).

Although it was well established that Ca^{2+} is a cofactor for the water splitting reaction [35] there were few attempt to speculate how this metal ion may be located in the catalytic centre relative to the Mn-cluster even though EXAFS analyses had provided evidence that it is located at a fixed distance from one or two Mn ions, estimated to be about 3.4 Å [20,24,36–38]. The application of X-ray crystallography not only rectified this and provided evidence for the 3 + 1 organisation of four Mn ions in PSII but also revealed details about the protein environment of these metal ions, information critically important for elucidating the chemistry of the water splitting reaction.

2. The structure of the Mn_4Ca-cluster derived from X-ray crystallography

2.1. Zouni et al. [52]

Although there had been considerable progress in determining the three-dimensional structure of PSII using electron microscopy, both electron crystallography [39–44] and single particle analyses [45–51], the spatial resolutions obtained were not sufficient to identify the electron density of the Mn_4Ca-cluster. This situation was rectified by subjecting 3D crystals of PSII, isolated from the cyanobacterium *Thermosynechococcus elongatus*, to X-ray diffraction analysis [52]. This analysis

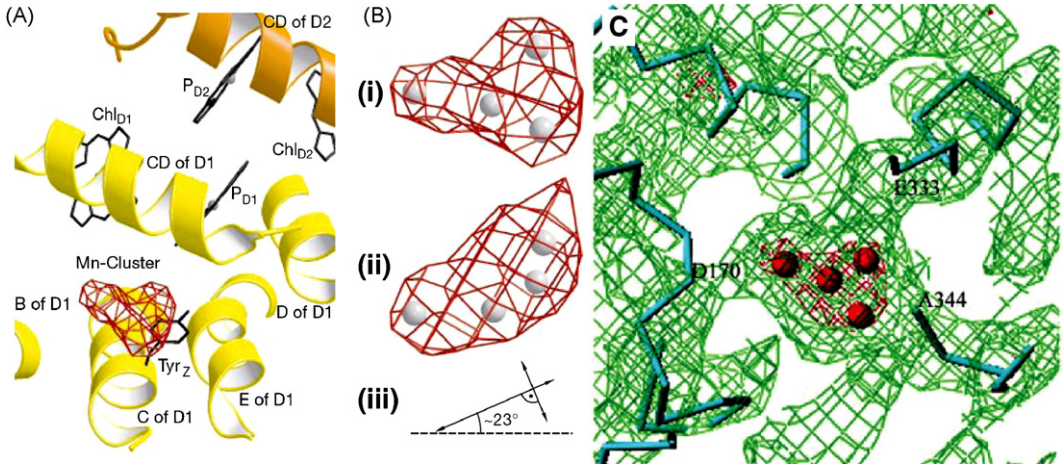

Fig. 1. Structure of the water splitting site from (a) Zouni et al. [52] and (b) Kamiya and Shen [56]. (A) A view of the water splitting site from the lumenal side onto the membrane plane, showing the electron density of the Mn-cluster contoured at 5σ. Also shown are the transmembrane helices, B–E of the D1 protein and the CD surface helices of the D1 and D2 proteins, side views of the P680 chlorophylls, P_{D1} and P_{D2} proteins, side views of the approximate position of D1Tyr161 (Tyr_Z). Reprinted by permission from Macmillan Publishers Ltd.: Zouni et al. [52]. (B) Enlargement of the electron density assigned to the Mn-cluster. (i) Viewed from the lumenal side onto the membrane plane, (ii) 90° rotated around the horizontal axis viewed along the membrane with the lumenal side on top. (iii) Orientation of the short and long axes of orientation (ii) showing that the cluster is tilted at 25° against the lumenal side of the membrane plane (broken line). Reprinted by permission from Macmillan Publishers Ltd.: Zouni et al. [52]. (C) View of the Mn-cluster and electron density surrounding it together with the assignment of the polypeptide chains. Some of the residues as possible ligands for the Mn-cluster are shown. Electron density of 5.0σ (red) and at 1.0σ (green). Copyright 2003 National Academy of Sciences, U.S.A.

generated an incomplete model of PSII at a resolution of 3.8 Å resolution: the tracing of C-alpha backbones of some subunits was not completed and there was no assignment of amino acids other than D1Tyr161 (Tyr_Z) and D2Tyr160 (Tyr_D). However the model confirmed the dimeric organisation of the isolated complex and the relative positioning of the major subunits and their transmembrane helices within each monomer previously derived from electron crystallography [53–55]. It also provided new information on the positioning of cofactors involved in excitation energy transfer and charge separation. Most importantly the analysis of the diffraction data revealed the first direct structural hints of the Mn-cluster (Fig. 1A). The electron density assigned to four Mn ions was checked by collecting anomalous diffraction data close to the Mn-absorption edge at 1.894 Å and was found to be towards the lumenal surface of PSII and to one side of the pseudo-two-fold axis which relates the transmembrane helices of the D1- and D2-reaction centre proteins and the cofactors they bind. In this way the location of the Mn-cluster breaks the pseudo-two-fold symmetry of the PSII reaction centre being located in the vicinity of the redox active Tyr161 of the D1 protein (Yz) and close to the surface helix located in the loop joining the lumenal ends of the C- and D-transmembrane helix of the D1 protein (CD-helix). The electron density had a "pear-shape" when contoured at 5σ having dimensions of 6.8 Å × 4.9 Å × 3.3 Å with the long axis approximately parallel to the CD-helix and tilted at about 23° to the membrane plane (see Fig. 1B). Because of the low resolution and incompleteness of the model, including the absence of side chain positioning, the assignment of Mn ions within the density was rather arbitrary. A Mn ion was positioned in the three bulges of the "pear-shaped" density to form an isosceles triangle with a fourth Mn ion placed in the centre of the triangle. The distance between the Mn ions was about 3 Å and therefore approximately consistent with EXAFS analyses [24]. However these workers did not propose a position for Ca^{2+} or model bridging ligands. Although the coordinates for the model were deposited (PDB 1FE1), no structural factors were supplied and therefore it has not been possible to reconstruct the electron density map derived from the analyses of Zouni et al. [52] and thus independently create a model.

2.2. Kamiya and Shen [56]

The 3 + 1 organisation of the four Mn ions modelled by Zouni et al. [52] gave support to the arrangement suggested by EPR studies [17,28,29] and was also a feature of the crystallographic model of the Mn-cluster derived by Kamiya and Shen [56]. Using PSII isolated from *Thermosynechococcus vulcanus*, a cyanobacterium closely related to *T. elongatus*, these workers obtained a crystal structure at 3.7 Å and provided additional information to that revealed by Zouni et al. [52]. The tracing of main chains was more complete and there was some effort made to assign amino acids, particularly those of the D1 and D2 proteins, based in part on analogy with the structure of the L- and M-subunits of the reaction centre of purple bacteria, as well as to some regions of the chlorophyll-binding proteins, CP43 and CP47. With the exception of one additional chlorophyll bound to CP47, the positioning of cofactors was essentially the same as that reported by Zouni et al. [52] but Kamiya and Shen also assigned density for two closely located carotenoid molecules on the D2 side of the reaction centre. As found by Zouni et al. [52], the shape of the electron density for the Mn-cluster was "pear-shaped" when contoured at 5σ indicative of the 3 + 1 organisation (see Fig. 1C). However, Kamiya and Shen modelled the four Mn ions so that they were approximately in the same plane whereas Zouni et al. [52] had placed the central Mn ion protruding towards the lumenal surface. Importantly, Kamiya and Shen's map contained electron density connecting to that of the Mn-cluster (see Fig. 1C) that could be tentatively assigned to side chains of the D1 protein, including Ala344, Asp170, Glu333 (or His332). Mutagenesis studies already supported the idea that these residues could be ligands for the Mn ions [57,58] and the X-ray diffraction derived model confirmed the concept that the C-terminus of the D1 protein was intimately associated with the Mn-cluster [59]. Kamiya and Shen [52] also suggested that, based on weak electron density, D1His337, D1Asp189 (or D1His190) and D1Tyr73 may also be coordinated to Mn ions of the cluster.

As in the case of the earlier crystal structure [52], the model of Kamiya and Shen did not include a Ca^{2+} bound close to the Mn-cluster and was only partially refined. Also these workers did not report their structure factors when depositing the coordinates (PDB 1IZL) making it impossible for others to access the electron density map used to construct their model.

2.3. Ferreira et al. [60]

The first complete and refined structure of PSII came from the work of Ferreira et al. [60]. This 3.5 Å model not only gave the structures of the 19 different subunits of the *T. elongatus* PSII complex (except for one low molecular weight intrinsic subunit tentatively assigned to PsbN) but provided the first reliable information about the protein environments of all the major cofactors of PSII, particularly that of the Mn_4Ca^{2+}-cluster. Anomalous diffraction was collected at a wavelength of 1.89 Å to obtain an electron density profile for the Mn ions and at 2.25 Å to locate Ca^{2+} (at 2.25 Å calcium has an anomalous difference of almost four times stronger than Mn) (Fig. 2A). The anomalous difference diffraction data were made available in the database at the time of depositing the coordinates and structure factors (PDB 1S5L). Again the electron density attributed to the four Mn ions was "pear-shaped" indicative of the 3 + 1 organisation. However it is difficult to make a direct comparison with the corresponding density reported in the earlier crystal structures due to the unavailability of primary data. The Mn-anomalous difference map of Ferreira et al. correlated with one metal in the small domain and three in the large globular domain, whereas the 2.25 Å wavelength map covers one metal ion in the large domain. In this way three Mn ions and the Ca^{2+} where modelled as a trigonal pyramid with the Ca^{2+} at its apex, all located in the large domain. The fourth Mn was placed in the small domain.

The much improved quality of the electron density map led to the assignment of virtually all the amino acids in the

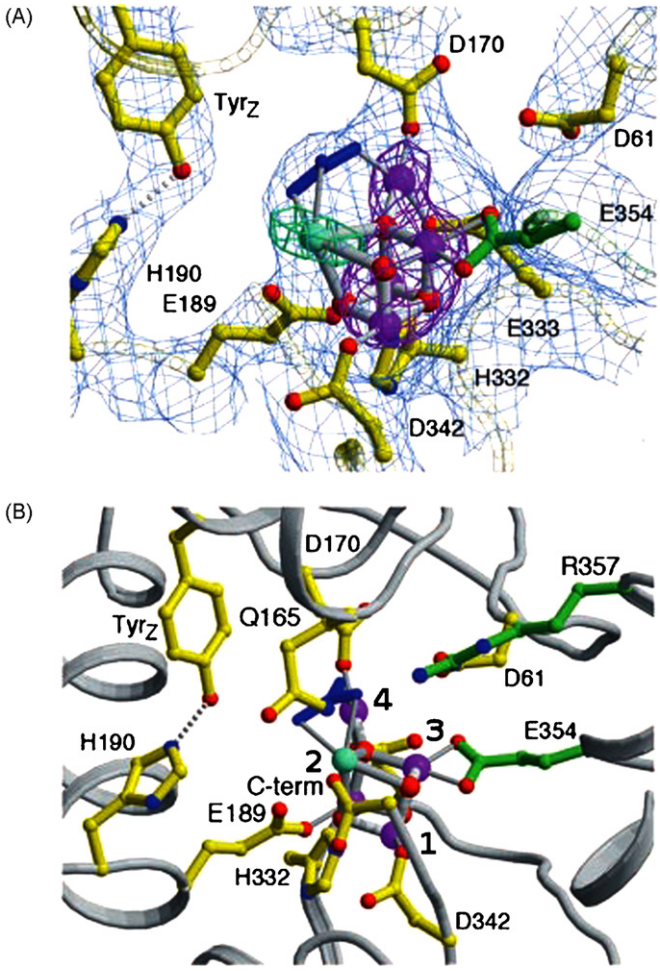

Fig. 2. Structure of the water splitting site from Ferreira et al. [60]. (A) View of the metal cluster with side chain ligands and (B) with possible catalytically important side chain residues. Mn ions, Ca^{2+} and oxygen atoms are shown in magenta, cyan and red, respectively. One unidentified non-protein ligand to the OEC and modelled as carbonate is coloured in blue. Protein main chain is depicted in light grey while the side chain bonds and carbon atoms follow the colouring of the protein subunits (D1: yellow, CP43: green). In (A), σ_A weighted $2|F_o| - |F_c|$ density is shown as a light blue wire mesh contoured at 1.5σ. Anomalous difference Fourier maps at 1.89340 Å (Mn edge, contoured at 10σ) and 2.25430 Å (highlights Ca^{2+}, contoured at 7σ), wavelengths are shown in magenta and blue-green, respectively. From Ferreira et al. [60]. Reprinted with permission from AAAS.

PSII complex and in particular those in close proximity to the Mn_4Ca^{2+}-cluster. The positioning of side chains, the analyses of the anomalous diffraction data and recognition that the metal ions were likely to be bridged by oxo-bonds at distances suggested by EXAFS resulted in a detailed model for the Mn_4Ca^{2+}-cluster. The working model proposed by Ferreira et al. [60–62] consisted of the three Mn ions (Mn1, Mn2 and Mn3) forming a cubane-like arrangement with the Ca^{2+} linked by oxo-bonds. The fourth Mn (Mn4, the "dangler" of Peloquin et al. [29]) was suggested to be linked to the $Mn_3Ca^{2+}O_4$-cubane via the oxygen of one its oxo-bonds (see Fig. 2A). At the resolution of data, the precise positioning of the metal ions could not be determined. Therefore for simplicity the distances between the Mn ions in the cubane were taken as 2.7 Å with the Mn–Ca^{2+} distance in the cubane modelled at 3.4 Å. The dangler Mn was positioned 3.3 Å from the closest Mn ions of the cubane and about 4 Å from the Ca^{2+}. As a consequence the model would predict three Mn–di-μ-oxo–Mn bonds at 2.7 Å, three Mn–di-μ-oxo–Ca^{2+} bonds at 3.4 Å and two Mn–mono-μ-oxo–Mn bonds at 3.3 Å. Although the distances chosen were compatible with distances derived from EXAFS for the PSII metal cluster [20,24] the predicted numbers of each type of bond was not. Nevertheless, density function calculations [63,64] and chemical synthesis of a mixed Mn/Ca complex [65] suggested that such an organisation was chemically feasible despite there being no known similar structure in biology. Moreover the arrangement of the Mn ions was consistent with one of the possible models suggested from EXAFS [20] but their positioning differed to that proposed by Zouni et al. [52] and Kamiya and Shen [56]. A regular cubane structure for all four Mn ions had been proposed some time ago [66] and in more recent times Dismukes and colleagues [30] had suggested that a distorted form of a Mn_4O_4-cubane formed during the latter stages of the catalytic cycle leading to dioxygen formation.

Despite the uncertainty of the precise positioning of Mn ions and Ca^{2+}, due to the limited resolution of the X-ray diffraction data, omit map calculations using simulated annealing and a slow cooling procedure carried out by Ferreira et al. were consistent with their proposed positioning of the cations within the structure, thus allowing a detailed discussion of the role of the protein environment in the overall coordination of the metal cluster (see Fig. 2). Based on this, the Mn_3CaO_4-cubane had four side chains as ligands: D1Asp342 to Mn1, D1Glu189 and D1His332 for Mn2 and CP43Glu354 for Mn3 (possibly bidentate). The identification of the glutamate of CP43 as a Mn-ligand was a surprise and is a residue of a conserved motif Gly-Gly-Glu-Thr-Met-Arg-Phe-Trp-Asp which forms a 3_{10} helix in the large extrinsic loop joining the lumenal ends of transmembrane helices V and VI of this protein. In addition to these four apparent protein ligands it was noted that the C-terminal residue of the D1 protein, D1Ala344 is located close to Ca^{2+} and that D1His337 could be hydrogen bonded to one of the bridging oxo-bonds of the cubane. Two side chain densities were available as ligands for the "dangler" Mn4 outside the cubane cluster. These were identified as D1Asp170 and D1Glu333 and also noted was that D1Asp61 might also function as a ligand via a bridging water molecule. Because the coordination number is usually six or seven for Ca^{2+} and five or six for Mn, then according to the Ferreira et al. model there must be additional non-protein ligands such as water molecules or hydroxides. However a higher resolution structure (2.5 Å or better) will be required to assign these. Nevertheless Ferreira et al. [60] did emphasise that there was non-protein electron density in the vicinity of Mn(4) and Ca^{2+} which they tentatively assigned to a bicarbonate ion that formed bridging ligands between the two metals (see Fig. 2). Moreover the positioning of this carbonate ion adjacent to the redox active D1Tyr161 (Tyr_Z) suggested that this could be the site for the binding of two substrate water molecules during the catalytic cycle leading to the formation of dioxygen. Also located in this potential catalytic site are D1Gln165 and CP43Arg357 (Fig. 2B) which may provide a hydrogen bond-

ing network for deprotonation of the substrate water molecules, while D1Asp61 is strategically located at the mouth of a polar channel which probably functions to facilitate the exit of protons to the lumenal surface. This channel is about 30 Å long and composed of side chains of the D1 protein (Asp61, Glu65), D2 protein (Lys317, Glu312) and the extrinsic PsbO protein (Asp158, Asp222, Asp223, Asp224, His228 and Glu114). As well as acting as a pathway for removing protons, it probably also provides a route for supplying water molecules to the active site where both functions are aided by a Ca^{2+} bound at the lumenal end of the channel ligated by PsbO residues, Glu114, His231 and Glu54 [67,68]. The work of Ferreira et al. also established that D1His190 was in hydrogen bonding distance to D1Tyr161 as required, and predicted, for the oxidation of the latter by the primary electron donor of PSII, P680, to generate the neutral tyrosine radical [69,70].

The model proposed by Ferreira et al. [60] has recently been analysed in considerable depth using density function QM/MM analysis [64]. The calculations assumed that the tentatively identified carbonate in the X-ray structure is replaced by a chloride ion in the active S1 state of the water splitting catalytic cycle and that the assigned protein ligands were complemented by water and hydroxyl ligands to satisfy the coordination requirements of the five metal ions. Despite these adjustments the calculated model for the metal cluster was remarkably similar to that proposed by Ferreira et al. and confirmed that it is a chemically stable structure even in the absence of protein ligands. Simulation of EXAFS spectra from the QM/MM model was also consistent with experimental spectra obtained from non-orientated samples.

3. Extending the model

3.1. Loll et al. [93]

The Mn_3CaO_4-cubane linked to a fourth Mn ion by a mono-μ-oxo bridge proposed by Ferreira et al., published in February 2004, provided a model which has been shown to be chemically realistic based on synthesis [65] and quantum mechanical calculations [63,64]. The assignment of the metal ligands was also consistent with a wide range of mutational studies mainly made in the cyanobacterium, *Synechocystis* sp. PCC 6803 [57,58]. For example, the involvement of the C-terminal domain of D1 protein in the assembly and stabilization of the Mn-cluster was first emphasised by Diner et al. [59,71] followed by several studies suggesting that D1Asp342 and Ala344 could be metal ligands. Site directed mutagenesis of D1Glu189, D1His332, D1Glu333 and D1His337 had all indicated that these residues were likely to be involved directly or indirectly in stabilizing the catalytic centre [57,58]. Moreover there had been several studies indicating that D1Asp170 provided a ligand for a high affinity binding site for Mn and was important for the assembly of the metal cluster [72]. A similar function has also recently been implicated to a lesser degree for D1Glu333 [73]. Thus the structural model provided by Ferreira et al. [60] has been used for in-depth discussions of the mechanisms of water splitting and dioxygen formation [74–78] as well as many other facets of PSII functioning [67,68,79–85]. However since the publication of the Ferreira et al. crystal structure in early 2004, new information has become available which should help to improve and refine our understanding of the organisation of water splitting site.

The FTIR studies of Debus and colleagues have questioned the assignment of some of the protein ligands [86,87]. Their detailed analysis of the vibrational properties of the carboxyl group of D1Ala344 on progressing from S1 to S2 suggested that this side chain forms a direct ligand to Mn ion of the cluster and not to Ca^{2+}, a conclusion also arrived at by others [88,89]. On the other hand no evidence was found for D1Asp170 [90] or D1Glu189 [91] being ligated to a Mn ion that underwent oxidation changes during the transitions from S0 to S1, S1 to S2 or from S2 to S3. In the case of D1Asp170 the FTIR result, of course, does not imply that D1Asp170 is not a Mn-ligand but is inconsistent with the notion that Mn4 is a key site for oxidation during S-state cycling [74,75,92].

Towards the end of 2005 a new crystal structure of PSII isolated from *T. elongatus* was published by Loll et al. [93] following on from an earlier study [94]. The resolution of the structure was reported to be 3.0 Å. In most part this new model confirmed the subunit and amino acid assignment and side chain positioning reported by Ferreira et al. [60] with most differences within the limitation imposed by the intermediate resolution of both structures. Nevertheless the improved electron density map allowed Loll et al. to extend and correct the original assignment of carotenoid molecules by Ferreira et al. and to locate several bound lipid molecules. As in the earlier papers from this group [52], the pear-shaped electron density attributed to the metal cluster of the water splitting site was interpreted as four Mn cations organised in a Y-shape or 3 + 1 arrangement (Fig. 3). Based on anomalous diffraction, the Ca^{2+} was placed in a position similar to that proposed by Ferreira et al. [60] whereas the positioning of three of the Mn ions was different to that of Ferreira et al. [60] but less so to that suggested by Zouni et al. [52] model. The fourth Mn ion was assigned to the narrow end of the pear-shaped density in a slightly different position to that of Ferreira et al. [60] or Zouni et al. [52]. The Loll et al. model for the metal cluster, like that of Ferreira et al. [60], had distances between the metal ions which were in line with those derived from EXAFS measurements [24]. They assumed di-μ-oxo bridges of 2.7 Å between Mn1 and Mn2 and between Mn2 and Mn3, while Mn1–Mn3 and Mn3–Mn4 were modelled at 3.3 Å as expected for mono-μ-oxo bridging (see Fig. 3).

The electron density surrounding the metals cluster was assigned to the same amino acids first identified by Ferreira et al. [60] although there were differences in the precise location in some cases (Fig. 3A). Loll et al., however, did not identify the electron density modelled as carbonate by Ferreira et al. [60]. Within the errors of the two models, Loll et al. confirmed the Ferreira et al. assignment of most of the key residues in the water splitting site such as D1Tyr161, D1His190, D1Glu165, D1Asp62, D1His337, CP43Arg357 and the likely metal ligands D1His332, D1Glu333, D1Glu189 and CP43Glu354. The most striking difference was the position of D1Asp170 and to a lesser extent D1Asp342 and D1Ala344. With these differences, Loll et al. proposed a coordination arrangement somewhat different to

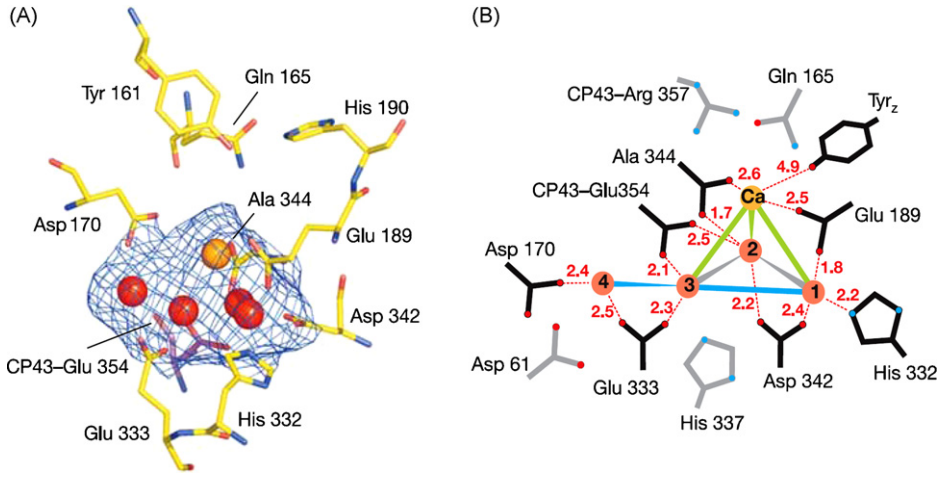

Fig. 3. Structure of the water splitting site from Loll et al. [93]. (A) Electron density of the Mn_4Ca^{2+}-cluster viewed along the membrane plane. The $2|F_o| - |F_c|$ map is contoured at 1.2σ and the colour coding is Mn (red), Ca^{2+} (orange), D1 side chains (yellow) and CP43 side chains (magenta). (B) Schematic view of the Mn_4Ca^{2+}-cluster with inter-connecting distances shown as lines; grey 2.7 Å, blue 3.3 Å and green 3.4 Å. Amino acids within the first coordination sphere of the metals and therefore proposed to be ligands are shown in black while those in the second coordination sphere are shown in grey. Distances are shown in Å. Reprinted by permission from Macmillan Publishers Ltd.: Loll et al. [93].

that provided earlier by Ferreira et al. The FTIR studies of Debus and colleagues [86,90] had indicated that D1Ala344 formed a ligand with a Mn ion which underwent an oxidation during the S1 to S2 transition and Loll et al. suggested that the carbonyl oxygens of this D1 terminal residue formed a bidentate bridge between Ca^{2+} and Mn2 which may convert to a monodentate Mn-ligand in higher S-states as suggested by Noguchi et al. [95]. They also proposed that D1Glu189 provided a ligand for Ca^{2+} as well as for Mn1. D1Asp342 was modelled as a bidentate bridging ligand to Mn1 and Mn2 while bidentate bridging between Mn3 and Mn4 was provided by D1Glu333. The carboxylate of CP43Glu354 was modelled with bidentate bridging between Mn2 and Mn3 while D1His332 provided a ligand to Mn1. However, Loll et al. emphasised that their model for the water splitting site schematically shown in Fig. 3B, was tentative, in part because of the low resolution of the electron density map and in part because of radiation damage. Working with the EXAFS group at Berkeley, and prior to the Loll et al. crystal structure, the same group had shown that doses of X-rays typical of those used for diffraction analyses caused the reduction of the Mn-cluster and associated structural changes [96]. This problem of radiation damage occurring at the Mn-cluster had also been highlighted by Dau et al. [97,98] and investigated further by Grabolle et al. [99]. Indeed, Loll et al. concluded that low Mn-anomalous difference density for Mn4 in their map was due to low occupancy brought about by radiation damage. This could account for the clear difference in positioning of D1Asp170, between the two structures.

Despite the uncertainties of the Ferreira et al. and Loll et al. models of the Mn-cluster due to radiation damage and differences in interpretation, the concept of bidentate bridging ligands proposed in the latter is worthy of serious consideration given

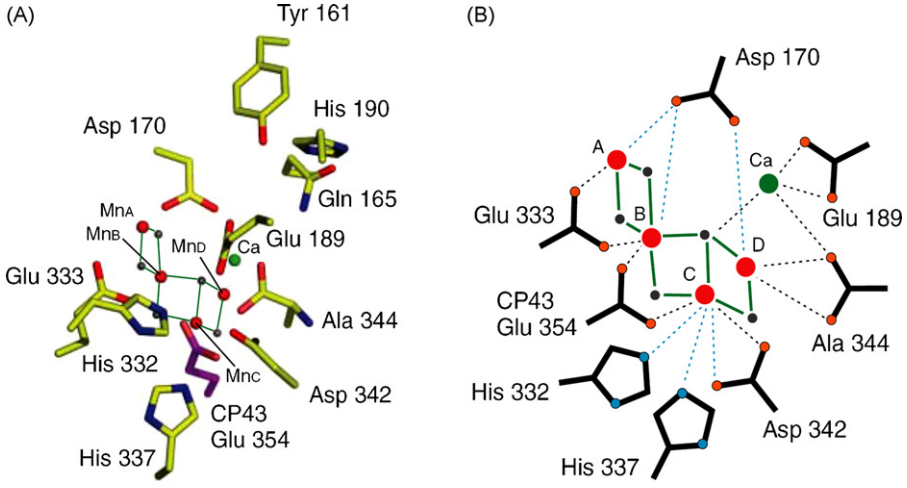

Fig. 4. Structure of the water splitting site from Yano et al. [104]. The organisation of the four Mn ions was derived from polarised EXAFS and 3D crystals of PSII from *T. elongatus* and is one of three possible arrangements (Model II). The protein environment was taken from the crystal structure of Loll et al. [93]. From Yano et al. [104]. Reprinted with permission from AAAS.

that this type of ligation is common in Mn-containing enzymes such as Arginase [100], *Escherichia coli* ribonucleotide reductase (for example Ref. [101]) and others (see Ref. [102]) and also in Mn-containing model compounds [103]. The presence of bridging carboxylate ligands may explain mutational studies where the replacement of some of the proposed ligands with non-ligating side chains does not disrupt the cluster and inhibit water oxidation [57,58].

3.2. Yano et al. [104]

To date the X-ray diffraction studies have made an enormous contribution to our understanding of PSII and, although limited by spatial resolution, has told us a great deal about the nature of the water splitting site and provided a structural basis for revealing the elusive and intriguing chemistry by which two substrate water molecules are oxidised to dioxygen. Of course the challenge is to improve the resolution of the X-ray diffraction data so as to identify the individual metal ions, disclose the nature of the low molecular weight species in their vicinity, including the substrate water molecules, and to obtain this information for different stages of the S-state cycle. At present the models for the Mn_4Ca^{2+}-clusters have relied heavily on metal–metal distances measured by EXAFS. Interestingly it is this technique which has emphasised the uncertainties of the models derived to date from X-ray crystallography.

As pointed out in a recent paper by Yano et al. [96] and Dau and colleagues [97–99], EXAFS can be employed using low doses of X-rays and therefore minimizes the type of radiation damage generated while collecting X-ray diffraction data. With this in mind Yano et al. [104] have used polarised X-ray spectroscopy to investigate the organisation of the Mn_4Ca^{2+}-cluster in crystals of PSII isolated from *T. elongatus* using levels of radiation where little or no reduction of Mn ions occurs. From this study, four different models for the Mn_4Ca^{2+}-cluster were derived (I, II, IIa and III). In themselves these models have limited value for elucidating the precise details of the water splitting reaction, unless they are introduced into the protein environment which constitutes the catalytic site, a procedure which is not straightforward because there are four possible symmetry-related orientations of each model and because of the possible radiation induced modification of the crystal structures of the metal-binding site. Nevertheless, Yano et al. proceeded to combine the EXAFS modelling with structural details derived from X-ray crystallography [104]. They therefore accepted that the electron density of the Mn_4-cluster was "pear-shaped" that the Ca-binding site was located in the approximate position as proposed by Ferriera et al. [60] and confirmed by Loll et al. [93] and that the assignment of the side chains were as in Loll et al. [93]. This resulted in four different models for the catalytic site which were different to those modelled from X-ray crystallography [60,93] with Model II chosen for a more detailed description in the main paper (see Fig. 4). Bearing in mind the tentative nature of the fitting and possible modifications in side chain positions due to radiation damage, the ligation pattern is very different to that proposed by Ferreira et al. [60] and Loll et al. [93]. For example D1Asp170 is no longer a direct ligand to MnA (equivalent to Mn4) and D1Glu189 becomes a bidentate ligand to Ca^{2+}. D1Ala344 seem to form bidentate ligand for MnD while D1Asp342 may provide a monodentate ligand to MnC. According to this model, neither D1His332 nor D1His337 are in ligating distance to a Mn ion. Only D1Glu333 and CP43Glu354 were positioned so as to possibly form bidentate bridging ligands, the former for MnB (equivalent to Mn3) and MnA and the latter between MnB and MnC.

Details of the introduction of the other EXAFS Models I and III into the crystal structure of Loll et al. were presented in the supporting online material for Yano et al. [104] but as expected this led to tentative ligation patterns different to Model II emphasising the lack of a unique EXAFS model and the uncertainty of combining data derived from EXAFS and X-ray diffraction at present.

3.3. Alternative interpretations

Clearly the structures of the water splitting site involving the introduction of the EXAFS models of Yano et al. [104] into X-ray diffraction derived electron density maps must be treated with caution, not only because there are four different EXAFS models to choose from but because of the limited resolution of the crystallographic data and its possible distortion by radiation damage. Nevertheless, we have undertaken alternative interpretations of the structure of the $Mn_4Ca^{2+}O_4$-cluster and its protein environment using currently available information and in particular the Mn-anomalous diffraction data of Ferreira et al. [60] which seems to be the most reliable at present and is available via the pdb database. Although this anomalous diffraction data is at 3.8 Å it has the advantage of not being biased to the model phases. The two models presented below have been fitted by real-space refinement against the anomalous diffraction using the molecular graphics programme, Coot [105]. Their validity will ultimately have to be reconciled with native electron density maps and higher resolution data.

3.3.1. Model 1

Our first approach was to modify the model of Ferriera et al. [60] by recognising that although EXAFS spectroscopy conducted by the Berkeley group[1] indicates that there are three Mn–di-μ-oxo bridges, there is likely to be only one mono-μ-oxo bridge [24,104]. Therefore one possibility that we consider here is that Mn4 is linked to $Mn_3Ca^{2+}O_4$-cluster via one of the Mn ions of the cubane (e.g. Mn3). Keeping the approximate positioning of Ca^{2+} proposed by Ferreira et al. [60], confirmed by Loll et al. [93] and recent work of Kargul et al. [106], then the new bonding state for Mn4 leads to a repositioning of the other three Mn ions as compared to those in the model of Ferreira et al. [60]. This repositioning of the Mn ions therefore changes

[1] There remains controversy in the literature regarding the numbers of Mn–mono-μ-oxo–Mn and Mn–di-μ-oxo–Mn bonds based on EXAFS measurements. For example, Dau and colleagues provide evidence for two, not three, Mn–di-μ-oxo–Mn bonds [97,98].

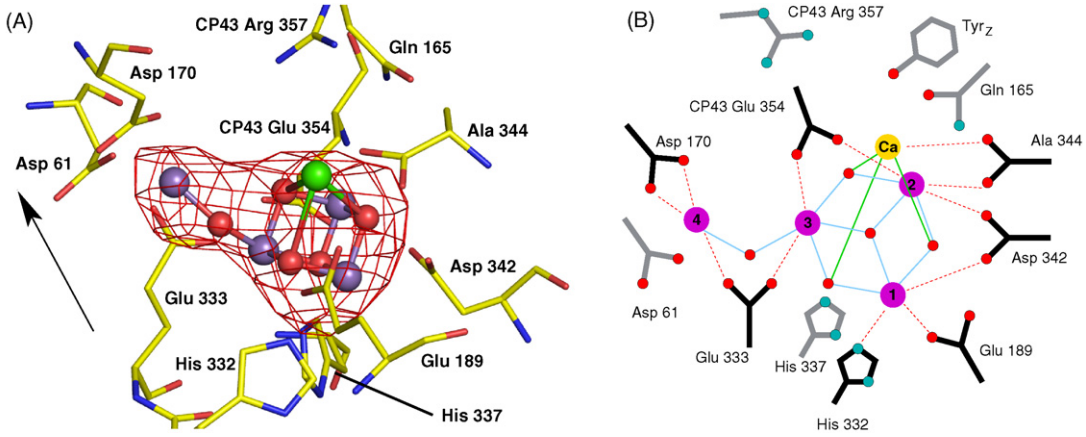

Fig. 5. Model 1. A refinement of the water splitting site using the electron density maps of Ferreira et al. [60] and Loll et al. [93] and Mn-anomalous difference map of Ferreira et al. [60], keeping the $Mn_3Ca^{2+}O_4$-cubane of Ferreira et al. but with Mn_4 linked to it via a single 3.3 Å mono-μ-oxo bridge. The model was constructed using the molecular graphics program Coot [105]. (A) Structure of the water splitting site assuming a single mono-μ-oxo bridge between Mn_4 (dangler Mn) and Mn_3 of the $Mn_3Ca^{2+}O_4$-cubane fitted with the Mn-anomalous difference map shown in red and contoured at 5.0σ. The amino acid assignments and the positioning of their side chains are based on the native electron density maps of Ferreira et al. [60] and Loll et al. [93] (see text). The arrow is in the direction of the normal of the membrane. (B) Schematic model shown in (A) with distance less than 2.8 Å shown as lines is indicative of the ligation pattern for this model. The CP43Arg 357 however, is about 4.5 Å away from Mn4. The inclusion of oxo bridging is in line with Mn chemistry and EXAFS measurements although other bridging ligands, such as OH should not be ruled out. (For interpretation of the references to colour in this figure legend, the reader is referred to the web version of the article.)

the protein ligation pattern as shown in Fig. 5. The positioning of the amino acids has taken into account the possibility of bidentate bridging coupled with slight changes in the side chain positioning within the native electron density maps derived by Ferreira et al. [60] and Loll et al. [93]. In this model the same amino acids identified by Ferreira et al. remain as metal ligands but the pattern is different: D1His332 is a ligand to Mn1 and D1Asp342 could now form a bidendate bridging ligation with Mn1 and Mn2. CP43Glu354 also seems to be positioned so as to form a bidentate bridge between Mn2 and Mn3. A repositioning of the side chain of D1Glu333, in agreement with Loll et al. [93], suggests that D1Glu333 could form a ligating bridge between Mn4 and Mn3. As mentioned above, the positioning of D1Asp170 is different in the Loll et al. structure compared with that of Ferreira et al. Assuming the Ferreira et al. positioning for D1Asp170 clearly makes this amino acid a ligand for Mn4 and with a slight rotation of the carboxylate bonds within the electron density suggests that both oxygens could ligate to Mn4. The positioning of the side chain of D1Glu189 suggests a monodentate ligation to Mn1 while re-interpreting the electron density of the C-terminal region of either the map of Ferreira et al. or Loll et al. is more difficult. It is clear that both D1Ala344 and D1Asp342 are located close to Mn2 and with slight adjustment of their side chains in either map could mean that the oxygens of the carboxyl groups of D1Ala344 form a bridge between Mn2 and Ca^{2+} while D1Asp342 forms a bidentate bridging ligand between Mn1 and Mn2. Fig. 5B shows a schematic representation of the ligation pattern for this model. Mn ions usually have coordination numbers of five or six and according to the model shown in Fig. 5 this requirement is better satisfied than in the Ferreira et al. [60] model due to introduction of bidentate ligation; six for Mn1, six for Mn2, six for Mn3 and four for Mn4. Any deficit in coordinating species is probably satisfied by low molecular weight species such as water and hydroxyl ions. The overall positioning of the Mn ions in this model and the pattern of amino acid ligation is similar to that proposed by Loll et al. [93] (see Fig. 3) with some exceptions. However the average orientation to the membrane normal of the three Mn–di-μ-oxo–Mn bonds (81°) and the Mn–mono-μ-oxo–Mn bond (47°) are not consistent with those recently derived from polarised EXAFS [96,104] which indicate 40–60° and 90°, respectively.

Although the major difference between the model shown in Fig. 5 and that of Ferreira et al. (Fig. 2) is the relocation of the Mn ions so as to accommodate only one Mn–mono-μ-oxo–Mn bond, the slight changes in the orientation of some side chains also makes some differences to the original Ferreira et al. model (Fig. 2): D1Ala344 is now in ligating distance to Mn2 as well as Ca^{2+} and bridging ligands are also proposed between Mn1 and Mn2 (D1Asp342), Mn2 and Mn3 (CP43Glu354) and between Mn3 and Mn4 (D1Glu333).

3.3.2. Model 2

The cubane model proposed by Ferreira et al. or its modified form proposed above (Fig. 5), or the Loll et al. model (Fig. 4), are not consistent with any of the four models recently proposed from polarised EXAFS spectroscopy as applied to single crystals [104]. We therefore have investigated the EXAFS models using the Mn-anomalous diffraction difference map derived by Ferreira et al. [60]. We found that none of the recently proposed EXAFS models fitted comfortably into the Mn-anomalous diffraction data using the coordinates provided [104]. However, in line with Yano et al. [104] we decided to focus on Model II and use real-space refinement against the anomalous Mn difference density to obtain a revised fitting. Recognising that there are discrepancies in the determination of the bond angles as emphasised by comparison of Yano et al. [104] with Pushkar et al. [107] as well as with earlier work [107–109], we slightly re-orientated the model so as to improve its fit within the Mn-

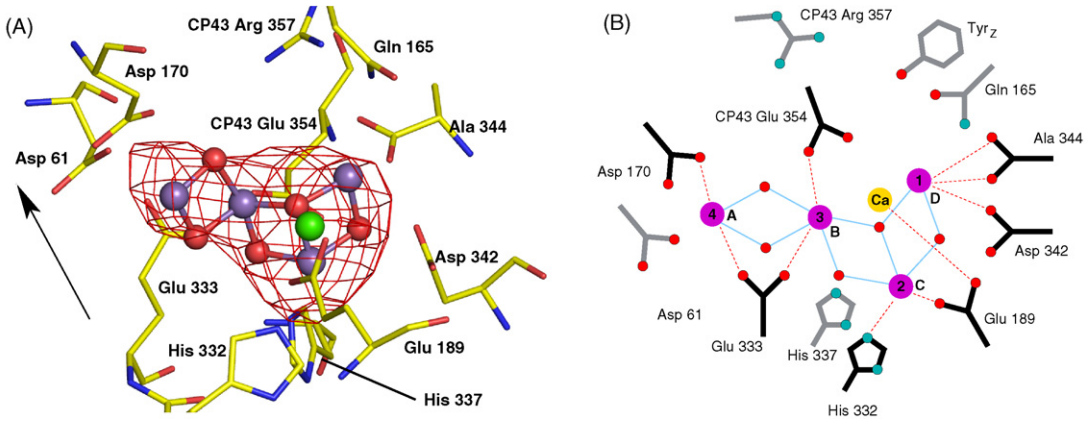

Fig. 6. Model 2. A refinement, using Coot [105], of the positioning of the EXAFS models (Model II) into the Mn-anomalous diffraction data of Ferreira et al. [60], maintaining the side chain positioning given in Fig. 4. (A) Model II of Yano et al. [104] was positioned into the Mn-anomalous difference map of Ferreira et al. [60] by adjusting the coordinates relative to the Loll et al. structure by lateral translation and rotation but maintaining the approximate orientation restraints provided by the recent EXAFS studies [104,107]. The arrow is in the direction of the normal of the membrane. (B) Schematic model shown in (A) with distance less than 2.8 Å shown as lines are indicative of the ligation pattern for this model.

anomalous difference map (see Fig. 6). This new fitting within the crystal structure gives an average orientation of the three Mn–di-μ-oxo–Mn to the membrane normal of about 55° and for the Mn–mono-μ-oxo–Mn bond of 87°, which are consistent with the corresponding EXAFS values determined with orientated thylakoid membranes [106] and with earlier estimates [108–110]. This new fitting of Model II into the Mn-anomalous diffraction data and the modified amino acid side chain positioning used in Fig. 5 gives a pattern of ligation shown in Fig. 6B. The pattern has some similarities to that proposed by Yano et al. [104] but there are some important differences; D1Asp170 now remains a ligand to Mn4 (MnA in Ref. [103])), D1Glu189 provides a bridge between Ca and Mn2 (MnC), D1Asp342 is a ligand for Mn1 (MnD) not Mn2 (MnC) and D1His332 is now in ligating distance to Mn2 (MnC).

4. Conclusion

In less than a decade, electron microscopy and X-ray crystallography have provided detailed information about the structure of PSII. The location and arrangement of the majority of the protein subunits of PSII have been revealed including the organisation of its transmembrane helices. X-ray crystallography of PSII isolated from cyanobacteria has provided the assignment of amino acids in these proteins as well as revealing the organisation of cofactors. Although the resolution has to date been restricted to 3.5–3.0 Å, the modelling of side chain positions suggests that, for the majority of the structure, there will only be slight modifications made to their position as the resolution of the X-ray data improves. Similarly this will be true for most of the cofactors. For this reason the current description of the protein environments around the various cofactors involved in energy transfer and charge separation is reliable. The main major uncertainties are the precise structure of the Mn_4Ca^{2+}-cluster and the exact details of its ligation, information paramount for fully elucidating the chemistry of the water splitting reaction.

However at present the crystal structures of PSII are not at a sufficient resolution to resolve the individual metal cations or the presence of low molecular weight ligands. The situation appears to be further complicated by the possibility that radiation damage occurs at the metal cluster during the collection of X-ray diffraction data. On the other hand information about the structure of the Mn_4Ca^{2+}-cluster can be obtained at high spatial resolution and with much reduced radiation damage by EXAFS spectroscopy. Recent EXAFS studies have not only confirmed earlier determinations on Mn–Mn and Mn–Ca^{2+} distances but imposed angular constraints for the metal–metal bonds relative to the membrane normal. Taken at face value these angular constraints invalidate the “cubane” models proposed by Ferreira et al. (Fig. 2 with two mono-μ-oxo bonds) and Model 1 presented in this paper (Fig. 5 with one mono-μ-oxo bond). Therefore, one of the four models derived from EXAFS studies of Yano et al. [104] could be considered to give a more realistic arrangement of the metal ions in the cluster and perhaps the proposed positioning within the crystal structure reported here (Fig. 6) provides an overall better working arrangement for EXAFS Model II. However, this modelling is only for one of four alternatives and is also open to criticism in terms of revealing the chemistry of the water splitting reaction, since it relies on X-ray diffraction data which may not be reliable because of radiation damage [96]. Moreover, the recent EXAFS work of Pushkar et al. [107] and earlier EXAFS studies [108–110] emphasise that there are significant discrepancies with the value determined by Yano et al. [104] for the average angle of the two 2.7 Å Mn–Mn bonds relative to the membrane normal. The new models discussed above (Figs. 5 and 6) and that of Loll et al. (Fig. 3) have introduced bidentate bridging and although this type of ligation is attractive, it is not favoured for metals in their high valency states. The coordinates for the two new models presented here in Figs. 5 and 6 are given in Ref. [111] where additional models based on the recent EXAFS work [104] are also considered.

The up-shot, therefore, is that although spectacular progress has been made towards elucidating the structure of the water splitting site of PSII by the application of X-ray crystallography, there remains a need to obtain higher resolution diffraction

data collected in such a way as to reduce radiation damage. The resolution must clearly identify water molecules with the view to identify those which act as the substrate during the catalytic cycle. This challenge, coupled with information derived from EXAFS, FTIR, EPR and other techniques, will ultimately provide the details required for understanding how photosynthetic organisms use sunlight to split water.

Acknowledgement

We wish to acknowledge the Biotechnology and Biological Research Council (BBSRC) for the financial support of this work.

References

[1] A. Pirson, Z. Bot. 31 (1937) 193.
[2] A. Pirson, C. Tichy, G. Wilhelmi, Planta 40 (1952) 199.
[3] B. Kok, G.M. Cheniae, in: R. Sanadi (Ed.), Current Topics in Bioenergetics, vol. 1, Academic Press, New York, 1966, p. 1.
[4] G.M. Cheniae, Annu. Rev. Plant Physiol. 21 (1970) 467.
[5] G.M. Cheniae, I.F. Martin, Plant Physiol. 50 (1972) 87.
[6] E. Kessler, W. Arthur, J.E. Brugger, Arch. Biochem. Biophys. 71 (1957) 326.
[7] R. Hill, F. Bendall, Nature 186 (1960) 136.
[8] D. Spencer, J.V. Possingham, Biochim. Biophys. Acta 52 (1961) 379.
[9] G.M. Cheniae, I.F. Martin, Brookhaven Symp. Biol. 19 (1966) 406.
[10] R.E. Blankenship, K. Sauer, Biochim. Biophys. Acta 357 (1974) 252.
[11] R. Radmer, G. Cheniae, in: J. Barber (Ed.), Primary Processes of Photosynthesis, Topics in Photosynthesis, Elsevier, The Netherlands, 1977, p. 303.
[12] G. Renger, W. Weiss, FEBS Lett. 137 (1982) 217.
[13] J.P. Dekker, J.J. Plijter, L. Ouwehand, H.J. van Gorkom, Biochim. Biophys. Acta 767 (1984) 176.
[14] H.T. Witt, E. Schlodder, K. Brettel, T.M. Saygin, Photosynth. Res. 10 (1986) 453.
[15] J. Lavergne, Biochim. Biophys. Acta 894 (1987) 91.
[16] G.C. Dismukes, Y. Siderer, Proc. Natl. Acad. Sci. U.S.A. 78 (1981) 274.
[17] J.M. Peloquin, R.D. Britt, Biochim. Biophys. Acta 1530 (2001) 96.
[18] C. Goussias, A. Boussac, A.W. Rutherford, Philos. Trans. R. Soc. B 357 (2002) 1369.
[19] D.B. Goodin, V.K. Yachandra, R.D. Britt, K. Sauer, M.P. Klein, Biochim. Biophys. 767 (1984) 209.
[20] J.H. Roblee, R.M. Cinco, V.K. Yachandra, Biochim. Biophys. Acta 1503 (2001) 7.
[21] H. Dau, L. Iuzzolino, J. Dittmer, Biochim. Biophys. Acta 1503 (2001) 24.
[22] V.K. Yachandra, K. Sauer, M.P. Klein, Chem. Rev. 96 (1996) 2927.
[23] J.E. Penner-Hahn, Struct. Bond. 90 (1998) 1.
[24] V.K. Yachandra, Philos. Trans. R. Soc. Lond. B 357 (2002) 1347.
[25] K. Sauer, J. Yano, V.K. Vachandra, Photosynth. Res. 85 (2005) 73.
[26] A.F. Miller, G.W. Brudvig, Biochim. Biophys. Acta 1056 (1991) 1.
[27] R.D. Britt, in: D.R. Ort, C.F. Yochum (Eds.), Oxygenic Photosynthesis, The Light Reactions, Kluwer, The Netherlands, 1996 (Chapter X).
[28] K. Hasegawa, T.A. Ono, Y. Inoue, M. Kusunoki, Chem. Phys. Lett. 300 (1999) 9.
[29] J.M. Peloquin, K.A. Campbell, D.W. Randall, M.A. Evanchik, V.L. Pecoraro, W.H. Armstrong, R.D. Britt, J. Am. Chem. Soc. 122 (2000) 10926.
[30] T.G. Carrell, A.M. Tyrshkin, G.C. Dismukes, J. Biol. Inorg. Chem. 7 (2002) 2.
[31] H.A. Chu, W. Hillier, N.A. Law, G.T. Babcock, Biochim. Biophys. Acta 1503 (2001) 69.
[32] K. Wieghardt, Angew. Chem. Int. Ed. 28 (1989) 1153.
[33] V.L. Peroraro, M.J. Baldwin, A. Gelasco, Chem. Rev. 94 (1994) 807.
[34] S. Mukhopadhyay, S.K. Mandal, S. Bhaduri, W.H. Armstrong, Chem. Rev. 104 (2004) 3981.
[35] R.J. Debus, Biochim. Biophys. Acta 1102 (1992) 269.
[36] M.J. Latimer, V.J. DeRose, I. Mukerji, V.K. Yachandra, K. Sauer, M.P. Klein, Biochemistry 34 (1995) 585.
[37] R.M. Cinco, J.H. Robblee, A. Rompel, C. Fernandez, V.K. Yachandra, K. Sauer, M.P. Klein, J. Phys. Chem. B 102 (1998) 8248.
[38] R.M. Cinco, K.L. McFarlane Holman, J.H. Robblee, J. Yano, S.A. Pizarro, E. Bellacchio, K. Sauer, V.K. Yachandra, Biochemistry 41 (2002) 12928.
[39] E.P. Morris, B. Hankamer, D. Zheleva, G. Friso, J. Barber, Structure 5 (1997) 837.
[40] K.-H. Rhee, E.P. Morris, D. Zheleva, B. Hankamer, W. Kühlbrandt, J. Barber, Nature 389 (1997) 522.
[41] K.-H. Rhee, E.P. Morris, J. Barber, W. Kühlbrandt, Nature 396 (1998) 283.
[42] B. Hankamer, E.P. Morris, J. Barber, Nat. Struct. Biol. 6 (1999) 560.
[43] B. Hankamer, E.P. Morris, J. Nield, C. Gerle, J. Barber, J. Struct. Biol. 135 (2001) 262.
[44] B. Hankamer, E.P. Morris, J. Nield, A. Carne, J. Barber, FEBS Lett. 504 (2001) 142.
[45] E.J. Boekema, B. Hankamer, D. Bald, J. Kruip, J. Nield, A.F. Boonstra, J. Barber, M. Rögner, Proc. Natl. Acad. Sci. U.S.A. 92 (1995) 175.
[46] J. Nield, E. Orlova, E. Morris, B. Gowen, M. van Heel, J. Barber, Nat. Struct. Biol. 7 (2000) 44.
[47] J. Nield, O. Kruse, J. Ruprecht, P. Da Fonseca, C. Büchel, J. Barber, J. Biol. Chem. 275 (2000) 27940.
[48] J. Nield, C. Funk, J. Barber, Philos. Trans. R. Soc. Lond. B 355 (2000) 1337.
[49] J. Nield, M. Balsera, J. De Las Rivas, J. Barber, J. Biol. Chem. 277 (2002) 15006.
[50] J. Barber, J. Nield, Philos. Trans. R. Soc. Lond. B 357 (2002) 1329.
[51] J. Nield, J. Barber, Biochim. Biophys. Acta 1757 (2006) 353.
[52] A. Zouni, H.T. Witt, J. Kern, P. Fromme, N. Krauss, W. Saenger, P. Orth, Nature 409 (2001) 739.
[53] B. Hankamer, J. Barber, E. Boekema, Annu. Rev. Plant Phys. Mol. Biol. 48 (1997) 641.
[54] J. Barber, Curr. Opin. Struct. Biol. 12 (2002) 523.
[55] J. Barber, Biophys. Q. Rev. 36 (2003) 71.
[56] N. Kamiya, J.R. Shen, Proc. Natl. Acad. Sci. U.S.A. 100 (2003) 98.
[57] R.J. Debus, Biochim. Biophys. Acta 1503 (2001) 164.
[58] B.A. Diner, Biochim. Biophys. Acta 1503 (2001) 147.
[59] B.A. Diner, P. Nixon, J.W. Farchaus, Curr. Opin. Struct. Biol. 1 (1991) 546.
[60] K.N. Ferreira, T.M. Iverson, K. Maghlaoui, J. Barber, S. Iwata, Science 303 (2004) 1831.
[61] J. Barber, K.N. Ferreira, K. Maghlaoui, S. Iwata, Phys. Chem. Chem. Phys. 6 (2004) 4737.
[62] J. Barber, S. Iwata, in: T. Wydrzynski, K. Satoh (Eds.), Photosystem. II. The Water Plastoquinone Oxido-reductase in Photosynthesis, Kluwer, The Netherlands, 2005, p. 469.
[63] M. Lundberg, P.E.M. Siegbahn, Phys. Chem. Chem. Phys. 6 (2004) 4772.
[64] E.M. Sproviero, J.A. Gascon, J.P. McEvoy, G.W. Brudvig, V.S. Batista, J. Chem. Theory Comput. 2 (2005) 1119.
[65] A. Misra, W. Wernsdorfer, K.A. Abboud, G. Christou, Chem. Commun. (2005) 54.
[66] J.C. De Paula, W.F. Beck, G.W. Brudvig, J. Am. Chem. Soc. 108 (1986) 4002.
[67] J.W. Murray, J. Barber, Biochemistry 45 (2006) 4128.
[68] J.W. Murray, J. Barber, J. Struct. Biol. 159 (2007) 228.
[69] C.W. Hoganson, G.T. Babcock, Science 277 (1997) 1953.
[70] C. Tommos, G.T. Babcock, Acc. Chem. Res. 31 (1998) 18.
[71] B.A. Diner, D.F. Ries, N.B. Cohen, J.G. Metz, J. Biol. Chem. 263 (1988) 8972.
[72] P.J. Nixon, B.A. Diner, Biochemistry 31 (1992) 942.
[73] R.O. Cowen, P.J. Nixon, B.A. Diner, J. Biol. Chem. 282 (2007) 7209.
[74] J.P. McEvoy, G.W. Brudvig, Phys. Chem. Chem. Phys. 6 (2004) 4754.
[75] J.P. McEvoy, J.A. Gascon, V.S. Batista, G.W. Brudvig, Photochem. Photobiol. Sci. 4 (2005) 940.

[76] G. Ananyev, T. Nguyen, C. Putnam-Evans, G.C. Dismukes, Photochem. Photobiol. Sci. 4 (2005) 991.
[77] P.E.M. Siegbahn, M. Lundberg, Photochem. Photobiol. Sci. 4 (2005) 1035.
[78] P.E.M. Siegbahn, Chem.: Eur. J. 12 (2006) 9217.
[79] C. Moser, C.C. Page, P.L. Dutton, Photochem. Photobiol. Sci. 4 (2005) 933.
[80] J. De Las Rivas, J. Barber, Photosynth. Res. 81 (2004) 329.
[81] J.W. Murray, J. Duncan, J. Barber, Trends Plant Sci. 11 (2006) 152.
[82] H. Ishikita, W. Saenger, B. Loll, J. Biesiadka, E.-W. Knapp, Biochemistry 45 (2006) 2063.
[83] S. Vasil'ev, D. Bruce, Plant Cell 16 (2004) 3059.
[84] S. Vasil'ev, D. Bruce, Biophys. J. 90 (2006) 3062.
[85] A. Telfer, Photochem. Photobiol. 4 (2005) 950.
[86] H.A. Chu, W. Hillier, R.J. Debus, Biochemistry 43 (2004) 3152.
[87] M.A. Strickler, L.M. Walker, W. Hillier, R.J. Debus, Biochemistry 44 (2005) 8571.
[88] Y. Kimura, N. Mizurawa, T. Yamanari, A. Ishii, T.A. Ono, J. Biol. Chem. 208 (2005) 2078.
[89] H. Suzuki, Y. Taguchi, M. Sugiura, A. Boussac, T. Noguchi, Biochemistry 45 (2006) 13454.
[90] R.J. Debus, M.A. Strickler, L.M. Walker, W. Hillier, Biochemistry 44 (2005) 3152.
[91] M.A. Strickler, W. Hillier, R.J. Debus, Biochemistry 45 (2006) 8801.
[92] J. Barber, in: D. Phillips, J. Barber (Eds.), The Life and Scientific Legacy of George Porter, Imperial College Press, London, 2006, p. 529.
[93] B. Loll, J. Kern, W. Saenger, A. Zouni, J. Biesiadka, Nature 438 (2005) 1040.
[94] J. Biesiadka, B. Loll, J. Kern, K.D. Irrgang, A. Zouni, Phys. Chem. Chem. Phys. 6 (2004) 4733.
[95] T. Noguchi, T. Ono, Y. Inoue, Biochim. Biophys. Acta 1228 (1995) 189.
[96] J. Yano, J. Kern, K.-D. Irrgang, M.J. Latimer, U. Bergmann, P. Glatzel, Y. Pushkar, J. Biesiadka, B. Loll, K. Sauer, J. Messinger, A. Zouni, V.K. Yachandra, Proc. Natl. Acad. Sci. U.S.A. 102 (2005) 12047.
[97] M. Haumann, C. Muller, P. Liebisch, L. Iuzzolino, J. Dittmer, M. Grabolle, T. Neisius, W. Meyer-Klauke, H. Dau, Biochemistry 44 (2005) 1894.
[98] H. Dau, P. Liebisch, M. Haumann, Phys. Chem. Chem. Phys. 6 (2004) 4781.
[99] M. Grabolle, M. Haumann, C. Muller, P. Liebisch, H. Dau, J. Biol. Chem. 281 (2006) 4580.
[100] Z.F. Kanyo, L.R. Scolnick, D.E. Ash, D.W. Christianson, Nature 383 (1996) 554.
[101] M. Sommerhalter, L. Saleh, J.M. Bollinger Jr., A.C. Rosenzweig, Acta Crystallogr. D: Biol. Crystallogr. 61 (2005) 1649.
[102] G.C. Dismukes, Chem. Rev. 96 (1996) 2909.
[103] G. Christou, Acc. Chem. Res. 22 (1989) 328.
[104] J. Yano, J. Kern, K. Sauer, M.J. Latimer, Y. Pushkar, J. Biesiadka, B. Loll, W. Saenger, J. Messinger, A. Zouni, V.K. Yachandra, Science 314 (2006) 821.
[105] P. Emsley, K. Cowtan, Acta Cryst. Sect. D: Biol. Cryst. 60 (2004) 2126.
[106] J. Kargul, K. Maghlaoui, J.W. Murray, Z. Deak, A. Boussac, A.W. Rutherford, I. Vass, J. Barber, Biochim. Biophys. Acta 1767 (2007) 404.
[107] Y. Pushkar, J. Yano, P. Glatzel, J. Messinger, A. Lewis, K. Sauer, U. Bergmann, V.K. Yachandra, J. Biol. Chem. 282 (2007) 7198.
[108] G.N. George, R.C. Prince, S.P. Cramer, Science 243 (1989) 789.
[109] J. Dittmer, H. Dau, J. Phys. Chem. B 102 (1998) 8196.
[110] H. Schiller, J. Dittmer, L. Luzzolino, W. Dorner, W. Meyer-Klauke, V.A. Sole, H.-F. Nolting, H. Dau, Biochemistry 37 (1998) 7340.
[111] J. Barber, J.W. Murray, Philos. Trans. R. Soc., in press.